# Automating Compression Ultrasonography of Human Thigh Tissue and Vessels via Strain Estimation

Rytis Jurkonis[1][a], Rimvydas Eitminavičius[1][b], Vaidotas Marozas[1][c] and Andrius Sakalauskas[2][d]
[1]*Biomedical Engineering Institute, Kaunas University of Technology, K. Baršausko 59, Kaunas, Lithuania*
[2]*TELEMED, Ultrasound Medical Systems, Savanoriu 178A, Vilnius, Lithuania*

Keywords: Deep Vein Thrombosis, Compression Quantification, Operator Free, Tissue Displacement.

Abstract: Despite the progress made in ultrasonic imaging, the current examination of vein structures by compression is highly operator-dependent and is a time-consuming clinical routine. Current guidelines for the management of deep vein thrombosis recommend compression ultrasonography follow-up for patients at risk of life-threatening complications (pulmonary embolism, heart attack, or stroke). New methods are needed to allow operator-free monitoring of vein structure at the point of care. This article presents the results of integrated imaging with a tissue compression actuator and automated control of tissue deformation through strain estimation. The data for feedback control of the actuator is calculated from raw ultrasound radio-frequency backscattered signals. The region-averaged strain curve (strain versus time) obtained during the tissue compression cycle serves as input for the actuator. The mounting on the human thigh is made from rigid, preshaped shells, which are adjusted to the circumference of the thigh with straps. The actuator facilitates a novel, on-body-mounted, automated, operator-free examination of the human femoral vein.

## 1 INTRODUCTION

Compression ultrasonography is a method for vein structure analysis, including testing of suspected deep vein thrombosis (DVT). DVT is the formation of a blood clot within the deep veins that blocks blood flow. In 50% of people with DVT, the clot eventually breaks off and travels to the central circulation, causing life-threatening complications (pulmonary embolism, heart attack, or stroke). Early diagnosis of DVT is crucial, and despite the progress made in ultrasonic imaging, the current examination of vein structures by compression is highly operator-dependent and a time-consuming clinical routine.

In reviewing the history of venous ultrasound, Cronan et al. (Cronan, 2003) mention that an article by Talbot et al. (Talbot et al., 1982) highlights a significant breakthrough in venous clot detection that occurred in 1982. Talbot noted that there were easily recognizable differences between patent normal veins and those containing clots. Using a combination of B-mode real-time imaging and pulsed Doppler imaging, the author indicated that (1) flows in a normal vein varied with respiration; (2) a Valsalva maneuver augmented the size of a normal vein; (3) light pressure exerted on a normal vein caused it to collapse; and (4) Doppler signals were found in a patent vein. Obstructed veins tend to be larger. Often, it contained a speckled mass within it, and the diameter did not change with respiration, a Valsalva maneuver, or light pressure exerted on the overlying skin. The next particular paper (Raghavendra et al., 1986) proposed a method called compression ultrasonography. Surprisingly, quantitative characterization of compression or criteria was described only in recent articles and only in cases of residual vein thrombosis. With sonography, vein diameters were evaluated during compression, and residual vein thrombosis (RVT) was defined as the persistence of thrombotic material resulting in a diameter of 4 mm or more (Prandoni et al., 2002). Criteria were defined as ultrasound incompressibility of at least 4 mm in the common femoral and/or popliteal vein after 3 months of RVT. This RVT criterion was shown to be reproducible in other institutions (Tan et al., 2012; Palareti et al., 2014; Liu et al., 2023).

[a] https://orcid.org/0000-0002-9481-1773
[b] https://orcid.org/0009-0009-4682-8878
[c] https://orcid.org/0000-0002-6879-5845
[d] https://orcid.org/0000-0002-3978-7301



Jurkonis, R., Eitminavičius, R., Marozas, V. and Sakalauskas, A.
Automating Compression Ultrasonography of Human Thigh Tissue and Vessels via Strain Estimation.
DOI: 10.5220/0013264300003911
Paper published under CC license (CC BY-NC-ND 4.0)
In *Proceedings of the 18th International Joint Conference on Biomedical Engineering Systems and Technologies (BIOSTEC 2025) - Volume 1*, pages 239-245
ISBN: 978-989-758-731-3; ISSN: 2184-4305
Proceedings Copyright © 2025 by SCITEPRESS – Science and Technology Publications, Lda.

To the best of the author's knowledge, no more quantitative criteria about the limits of compression are published. Therefore, there is a need for new objective criteria, especially from sonography images. The study explores the feasibility of automated compression ultrasonography of thigh tissues by proposing a hardware actuator and compression control solution. Results of the investigation (intra- and intersubject variability) by using the prototype are disclosed.

# 2 MATERIAL AND METHODS

## 2.1 Thigh Mount Supports

The prototype of the thigh mount was made from two rigid C-shaped frames (Fig. 1). When designing these C-shaped frames the anthropometric data (Heitmann and Frederiksen, 2009) of human thigh size (median circumference 56 cm) was considered. In one frame the locking slot for fixing the imaging transducer was formed according to the transducer enclosing dimensions. The first frame to the second was fixed with two nonelastic straps that were adjusted to the individual circumference of the thigh of the subject. After fixation, the length of the straps was stable during the time required for the whole session of data recording. The second C-shaped frame has two fixed bladders (Fig. 1 (b)). The fixation was made with woven fabric, for prototyping, while future support designs (including the choice of fabric materials) will be improved for better comfort of the user.

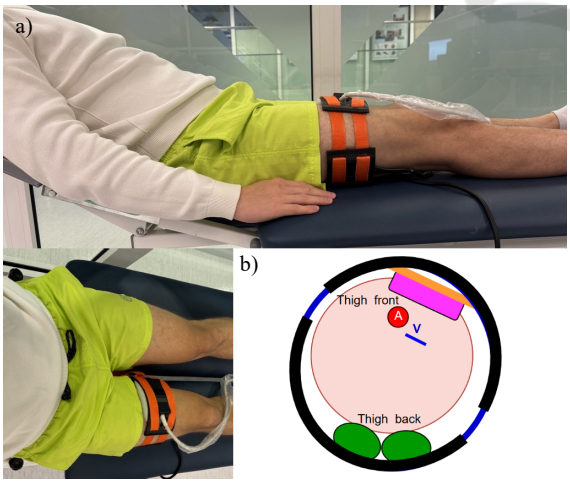



Figure 1: The tested design for mounting of compression actuator and imaging transducer on human thigh: a) mounting on the thigh; b) rigid frames with a mounted actuator pressing tissues against the imaging transducer. The approximate location of the femoral artery and the compressed femoral vein is indicated by "A" and "V", respectively.

## 2.2 Pneumatic Actuator

Actuation on tissues was performed using bladders that were in contact with the skin on the thigh. The air bladders were rectangular with a size of 60 x 100 mm. The required air volume to pressurize the bladders to 100 mmHg was 200 mL (per bladder). Bladders were pressurized by a silent piezoelectric air pump, model UXPB5400000A (Lee Company, Westbrook, CT, USA). This pump in combination with a smart pump module is capable of producing pressures of up to 190 mmHg, and a free flow output of 1.35 L/min. The pump and electronics were powered by a Li-Ion battery.

## 2.3 Ultrasonic Imaging

Thigh tissue imaging was performed using the ArtUs-1H beamformer (Telemed, Lithuania) that has raw beamformed radio frequency (RF) data output. The beamformer was equipped with a low-profile linear array (LF11-5H60-A3). The beamformer was interfaced to the computer via USB 3.0 and had synchronization output connectors installed. Sync pulses from the beamformer served as the activation signal for the pneumatic actuator. The main parameters of ultrasonic scanning were as follows: scanning depth of 5 cm, ultrasound wave frequency in the range of 5 - 11 MHz, and transmission of a single focal depth of 5 cm. B-mode images (512 x 512) were acquired in real-time into the host computer. The RF signal was digitized with a 40 MHz sampling frequency and the analog-to-digital converter resolution of 16 bits was analyzed in real-time as described in the 2.3.2 section.

### 2.3.1 Software

Two real-time streams—B-mode ultrasound images (for navigation) and RF data (for strain assessment)—were transmitted to the MATLAB environment and MATLAB GUI application using a software development kit (SDK) developed by TELEMED. The functionality of the MATLAB GUI application was sufficient for research purposes and had an option to: adjust imaging depth, choose the frequency of waves, adjust emission power and receiving gain, preset the threshold of strain, and initiate the imaging session. The DLL can be used to link C++ TELEMED SDK to any programming platform.

### 2.3.2 Estimation of Real-Time Tissue Axial Displacements and Strain

Tissue displacements and strain parameters (calculated from RF data) are well-known in the commu-

nity of ultrasound elastography (Garra, 2015). Typically, these parameters serve for the assessment of tissue hardening, because the parameters are highly correlated with the stiffness of tissue. In this study, tissue strain parameter was employed for the quantitative assessment of compression ultrasonography with implications to be used in the diagnosis of thrombotic veins. Axial displacements were estimated by using a window-based correlation technique proposed by Zahiri and Salcudean (Zahiri Azar and Salcudean, 2006). The algorithm is one of the fastest proposed up to date because it uses displacement value estimated in previous, neighboring, correlation window as a prior, to reduce the search for the next one to a very small area of 3 samples (-1, 0, +1). Displacement estimates are refined by using parabolic interpolation which is again very fast and efficient. The time delay was calculated by using the following parabolic interpolation formula:

$$\Delta = T_s \frac{y_0 - y_2}{2(y_0 - 2y_1 + y_2)} \quad (1)$$

where $T_s$ – ultrasound RF data sampling period, $y_1$ – the argument for maximal correlation (time delay for the correlation peak), and $y_0$, $y_2$ – nearest neighbors of the peak.

Strain estimates were obtained from displacements using a gradient operator combined with a smoothing filter. The size of the kernel for axial displacement evaluation was 107 (samples) × 7 (scan lines). The median value of the strain matrix is calculated from every frame of the RF data. Then the strain curve is formed from the calculated median values. Real-time strain assessment served in a feedback loop with a tissue compression actuator. The pneumatic actuator continuously applied the pressure onto the thigh gradually closing the vein under investigation at the same time strain was estimated for each received data frame of backscattered signals. The operator sets the strain threshold value in the MATLAB GUI application, which defines the end of the ultrasonic imaging session. At the instance when the imaging is stopped the beamformer provides a synchronization pulse to the actuator to halt the pump and initiate the release of the applied pressure.

## 2.4 Data Collection and Analysis

The subjects were instructed to relax their body muscles, similar to the procedure during blood pressure measurement with a brachial cuff. In addition, the positioning of the body and the leg was standardized: the subjects were placed on the testbed (Matsubara et al., 2022) with their back elevated at a 30-degree angle and the leg freely extended. Thigh tissue compressions were performed in two different variants: 1) manually, by maneuvering the imaging transducer, and 2) by using an automated tissue compression actuator. The automated compression was conducted with a thigh-mounted imaging transducer and pressurized bladders, as depicted in Figure 1. Manual compression was applied from the front side of the thigh, in the same way as in routine clinical practice. The dosing of compressions in both manual and automated variants was quantified using the preset strain thresholds in MATLAB GUI. Manual compression was stopped at 2, 5, 8, and 11% strain thresholds, while the automated compression was halted at 1.5, 2.5, 3.5, 4.5, and 5.5%. For each threshold, three compressions were recorded. These levels were chosen empirically based on a current design. Image sequences of tissue reactions were saved for off-line analysis, which is described in the following section.

The initial and final B-mode images from the single subject thigh compression session are provided in Fig. 2. In the initial image, the largest ellipse-shape darker pattern represents the femoral vein in cross-section. This pattern decreases in size as the thigh tissues are compressed, either manually or by the activated actuator. The artery lumen appears as a smaller, more circular pattern. The artery lumen begins to deform under a stronger compression, once the lumen of the healthy vein is fully closed. The depicted B-mode images are primarily used to initiate offline analysis (intermediate images are provided in the appendix Figure 9). M-mode imaging facilitated the analysis of deformation over time. To generate the M-mode image, the intensity of the B-mode image was extracted along the blue line, which is centered on the main vein width in the initial image (left panel in Fig. 2). The same line location is indicated on the B-mode image after maximal compression.

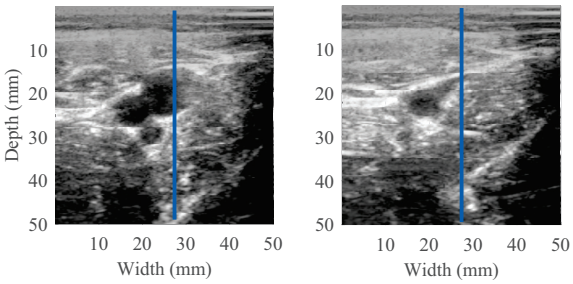



Figure 2: Cross-section B-mode images of femoral vessels before compression (left) and at full lumen closure of the veins (right).

The overview of tissue compression progress in a sequence of B-mode images can be enhanced by preparing M-mode images with a time dimension

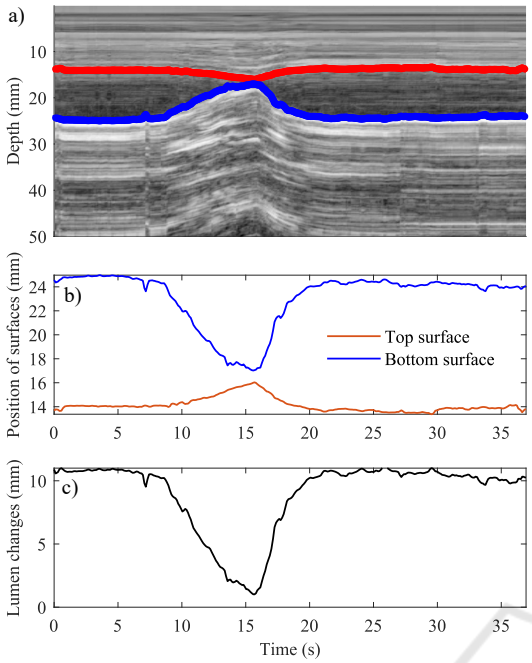



Figure 3: Human thigh imaging data: a) representation of vein lumen deforming in M-mode time diagram as prepared from image intensity profiles indicated on B-mode images; b) extracted position changes of vein walls (surfaces), and c) calculated vein lumen changes during compression and release of thigh tissues.

(Fig. 3 (a)). The transitions of tissue structures' positions appear more continuous and smooth, making tracking easier. Displacements of the upper and lower walls of the vein are extracted from the M-mode image, as exemplified by the lines on the grayscale image. These traces (Fig. 3 (b)) assist in calculating the absolute size of the vein lumen. Figure 3 (c) shows the initial size of the vein lumen, approximately 11 mm, which was compressed to around 1 mm, resulting in a relative decrease of the vein lumen by about 90%. This is an example of the resulting reaction of tissues and the femoral vein after manual compression on the thigh. The subjective quantification of the degree of compression could be enriched with strain parameter. The lumen decrease trace is exemplified together in strain–time dependency (Fig. 4).

The corresponding strain, as the quantity of the whole image, averaged degree of deformation, increases to more than 9% in the final stage of the compression. The strain increases while the lumen decreases, both peaking around 15 seconds in this example. The strain appears more smooth during compression and the release of the thigh. Strain value monitoring was done in real-time with ultrasonic imaging, allowing the degree of deformation to be dosed by the set threshold of strain. Real-time thresholding

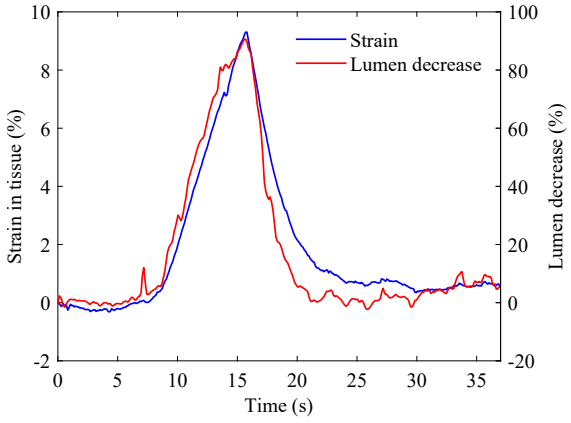



Figure 4: Comparison of lumen relative decrease with strain calculated from ultrasonic imaging RF data.

in strain trace was verified with vein lumen decrease obtained from the M-mode image. An example of the compression dosed according to the strain threshold is provided in Figure 5. In this example, the preset threshold for tissue strain was 8% which resulted in a vein lumen change from the initial size of 11.2 mm to 7.3 mm (relative decrease of 35%).

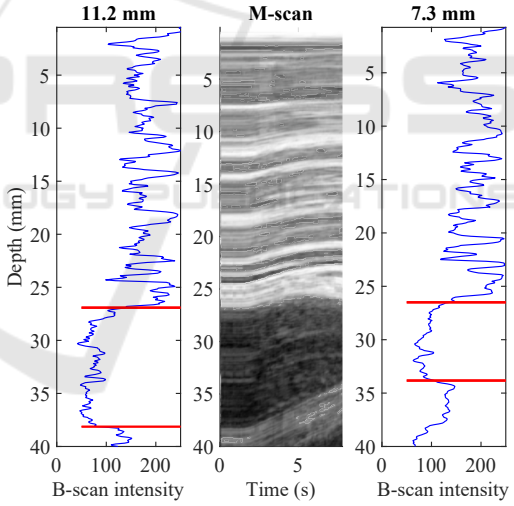



Figure 5: Analysis of the tissue compression image sequence: M-mode diagram is prepared for overview for overall progress; the B-mode image intensities profile exemplifies initial (left panel) and final (right panel) dimensions of vein lumen size.

This approach of estimation of only initial and final (strain threshold triggered) vein lumen sizes was applied in the analysis of data from a group of healthy subjects. In total three cases of thigh tissue reactions to compression were recorded and analyzed to estimate inter-subject variability. The possibilities of monitoring tissue reactions in single subjects, or intra-subject variability, were also evaluated.

## 3 RESULTS

In total 9 healthy volunteers were included in this study, all participating in the intersubject investigation and one of them in the long-term (2.5 hours) intrasubject investigation. Vein lumen responses to manual and automated compressions were analyzed offline in M-mode diagrams. Both inter-subject and intra-subject variabilities were examined. Figure 6 illustrates inter-subject variability in vein lumen reactions to manual and automated thigh compressions (intermediate images are provided in the appendix Figure 10 and Figure 11). Each point represents the mean result of three compression sessions, with lines connecting points to show trends for each subject.

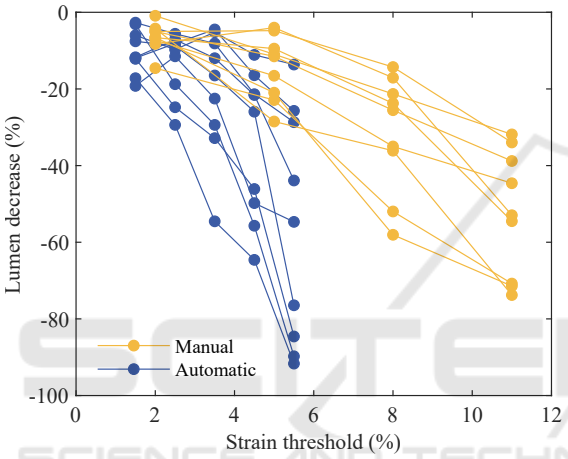



Figure 6: Reactions of vein lumen in healthy subjects with dosing the compression amount according to strain threshold: manual (by-hand) maneuvering and automatic compression.

Observed vein lumen reactions differ significantly. With the preset value of threshold of 11% for strain, vein lumen reduction can range from 30% to 70%. Meaning, that the same values of threshold can not be applied to a whole group. In the manual variant, the imaging transducer applies compression, while in the automatic variant, tissues are pushed toward it, causing the differences.

Figure 7 compares the results using boxplots for different strain thresholds in manual and automated compression ultrasonography procedures. A strong relationship between strain threshold and percentage of lumen decrease can be observed. However, the interquartile range of lumen decrease increases significantly at higher strain thresholds.

An automatic tissue compression actuator will be used for prolonged intermittent monitoring of venous conditions. Therefore, evaluating intra-subject variability in measurements is important. Figure 8 (a) presents two series of automatic measurements obtained using two different strain threshold settings over 150 minutes of monitoring. Figure 8 (b) compares the interquartile ranges of lumen decrease for these two strain threshold settings. A higher strain threshold setting results in significantly greater intra-subject variability in the estimated decrease in vein lumen.

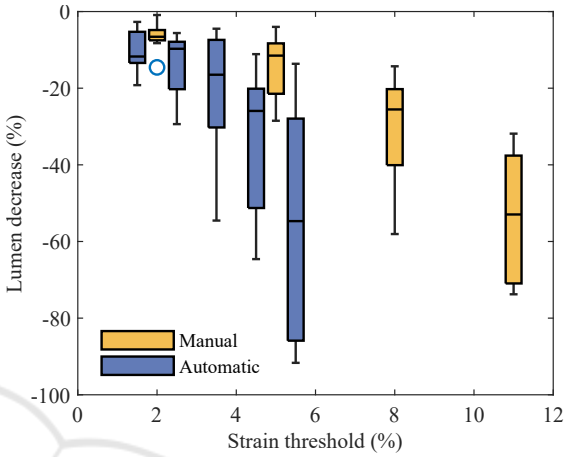



Figure 7: Box-plot of vein lumen decrements in healthy subjects during manual (by-hand) and automatic compression.

The boxplot in Figure 8 (b) provides a statistical representation of the data in Figure 8 (a). The notches do not overlap, which suggests a statistically significant difference in medians between the two groups. The left boxplot (2.5% threshold) has a much tighter interquartile range, indicating lower variability when compared to the right boxplot (4.5% threshold).

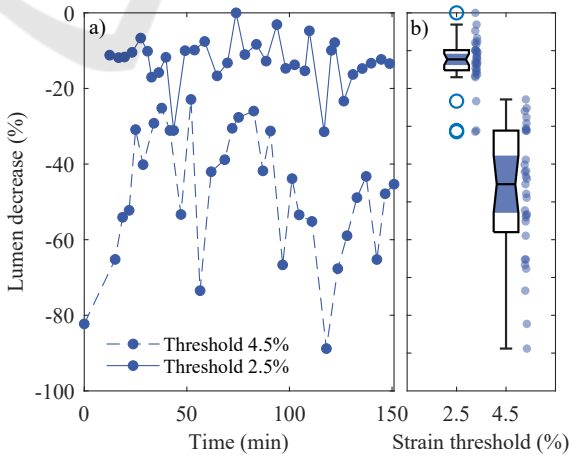



Figure 8: Results of vein lumen response using a thigh-mounted imaging transducer, with automated compression doses set to strain thresholds of 2.5% and 4.5%. A single actuator application produced 31 repeated automated compressions at each threshold over a 2.5-hour period.

SCITEPRESS SCIENCE AND TECHNOLOGY PUBLICATIONS

# 4 DISCUSSION

The tissue response to compression is subject-specific. Deformation and accordingly calculated strain depend on the site of actuation. If the actuator is mounted on the side with varying layers of adipose superficial tissue, or varying stiffness of muscle because of involuntary movements of the leg the reactions to compression will be different. So the intra-subject peculiarities of tissues are proposed to be considered with the initial adjustment of the strain threshold. The automatic compressions are performed from the back side of the thigh and result in smaller modulation of strain. Despite low modulation of strain, the actuation on the thigh from the opposite side and the use of rigid pre-shaped frames to mount the imaging transducer and actuating bladders contribute to reducing uncertainty in tissue response (reducing shear deformation).

The whole B-mode image was used for the strain estimate calculation and not justified to regions of thigh tissues. Adjusting region for strain estimation could potentially increase strain modulation and the accuracy in quantifying compression amount. Provided experimental results are from a limited number of healthy subjects. The personal body characteristics were not examined in detail, thus further research is needed including a bigger group of subjects with higher variability in body composition. Additionally, individualized calibration should be developed to perform long-term accurate monitoring of tissue response.

# 5 CONCLUSIONS

In this study, an ultrasonography tissue compression actuator for automated long-term monitoring of venous vessels in the lower extremities is proposed. The actuator is controlled by a tissue strain parameter that regulates compression. The results show a negative correlation between venous vessel lumen closure and the tissue strain parameter, suggesting that using tissue strain as a feedback mechanism is feasible. However, the variability at a higher strain threshold is relatively big, leaving room for improvement. Inter-subject variability could be addressed through initial calibration, while intra-subject variability for monitoring applications could be managed by defining a more targeted region of interest.

# ACKNOWLEDGEMENTS

This work is funded under the Horizon Europe Innovation Action ThrombUS+ (Grant Agreement No. 101137227), co-funded by the European Union.

# REFERENCES

Cronan, J. J. (2003). History of venous ultrasound. *J Ultrasound Med*, 22(11):1143–1146.

Garra, B. S. (2015). Elastography: history, principles, and technique comparison. *Abdom Imaging*, 40(4):680–697.

Heitmann, B. L. and Frederiksen, P. (2009). Thigh circumference and risk of heart disease and premature death: prospective cohort study. *BMJ*, 339:b3292.

Liu, Y., Deng, X., Zhu, F., Zhu, W., and Wang, Z. (2023). High fibrinogen and mixed proximal and distal thrombosis are associated with the risk of residual venous thrombosis in patients with posttraumatic deep vein thrombosis. *Front Cardiovasc Med*, 10:1003197.

Matsubara, S., Sugiyama, S., and Waki, N. (2022). Is long-axis or short-axis pulsed wave doppler optimal for preoperative assessment of varicose veins in the lower extremities? *The Japanese Journal of Phlebology*, 33:317–321.

Palareti, G., Cosmi, B., Legnani, C., Antonucci, E., De Micheli, V., Ghirarduzzi, A., Poli, D., Testa, S., Tosetto, A., Pengo, V., Prandoni, P., and DULCIS (D-dimer and ULtrasonography in Combination Italian Study) Investigators (2014). D-dimer to guide the duration of anticoagulation in patients with venous thromboembolism: a management study. *Blood*, 124(2):196–203.

Prandoni, P., Lensing, A. W. A., Prins, M. H., Bernardi, E., Marchiori, A., Bagatella, P., Frulla, M., Mosena, L., Tormene, D., Piccioli, A., Simioni, P., and Girolami, A. (2002). Residual venous thrombosis as a predictive factor of recurrent venous thromboembolism. *Ann Intern Med*, 137(12):955–960.

Raghavendra, B. N., Horii, S. C., Hilton, S., Subramanyam, B. R., Rosen, R. J., and Lam, S. (1986). Deep venous thrombosis: detection by probe compression of veins. *J Ultrasound Med*, 5(2):89–95.

Talbot, S. et al. (1982). Use of real-time imaging in identifying deep venous obstruction: a preliminary report. *Bruit*, 6(41-42):9.

Tan, M., Bornais, C., and Rodger, M. (2012). Interobserver reliability of compression ultrasound for residual thrombosis after first unprovoked deep vein thrombosis. *J Thromb Haemost*, 10(9):1775–1782.

Zahiri Azar, R. and Salcudean, S. (2006). Motion estimation in ultrasound images using time domain cross correlation with prior estimates. *IEEE transactions on bio-medical engineering*, 53:1990–2000.

# APPENDIX

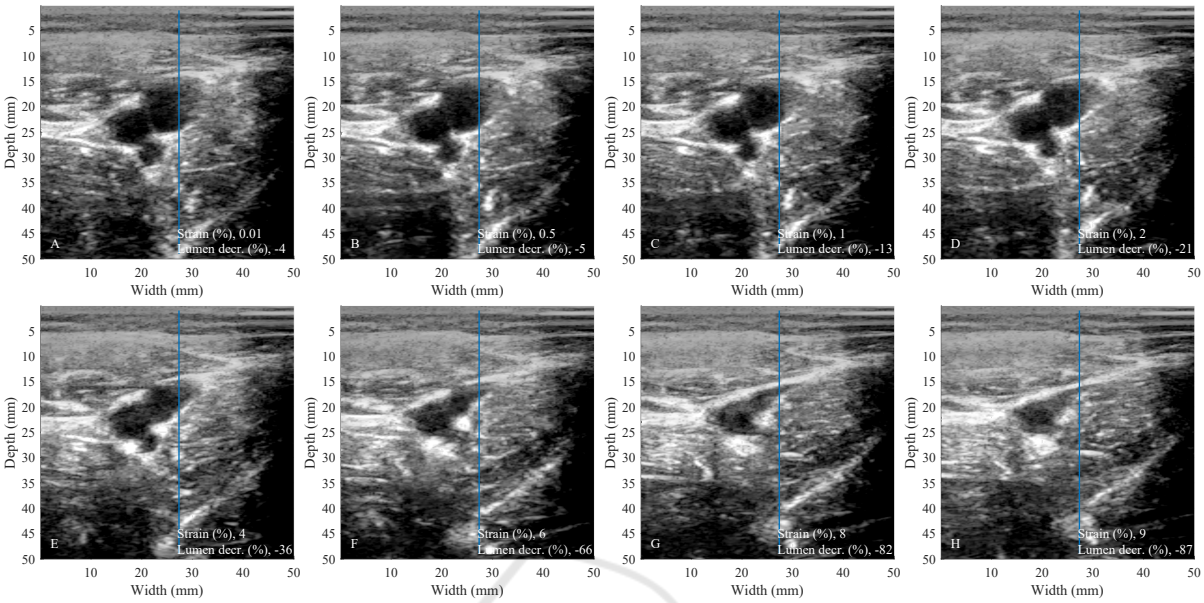



Figure 9: Cross-sectional images of femoral vessels during compression session of the thigh tissues. The artery is the most left circular pattern in all images and does not collapse at the end of the compression session.

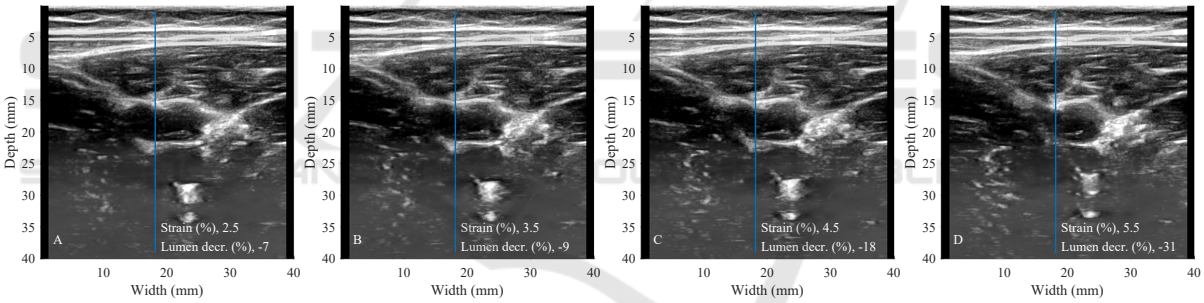



Figure 10: Cross-sectional images of blood vessels during automated compression (up to strain 5.5%) of thigh tissues: intermediate reactions of one of the subjects characterized in Figures 6.

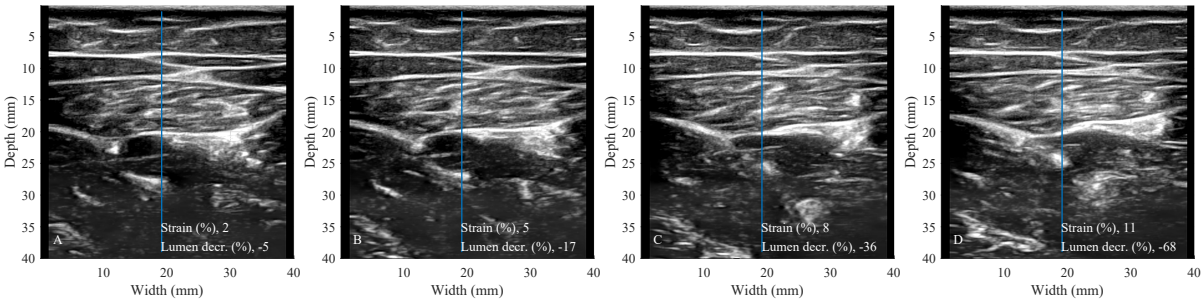



Figure 11: Cross-sectional images of blood vessels during manual compression (up to strain 11%) of thigh tissues: intermediate reactions of one of the subjects characterized in Figures 6.